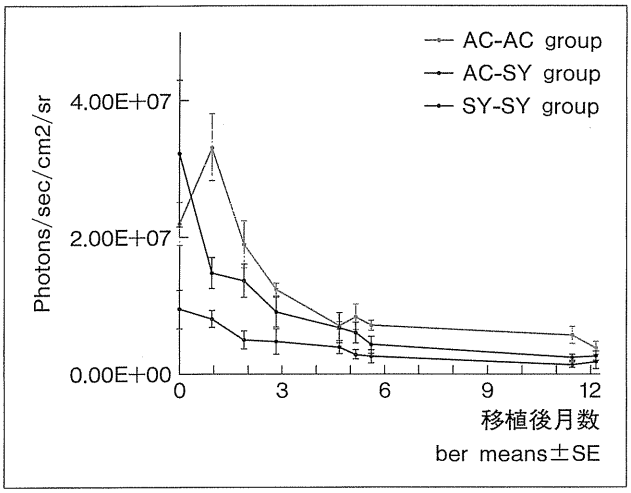

図4　細胞シート移植後の3群間の発光強度の推移
AC-AC group：Luc⁺軟骨細胞シート単独群
AC-SY group：Luc⁺軟骨細胞・Luc⁺滑膜細胞シート併用群
SY-SY group：Luc⁺滑膜細胞シート単独群

考察

BLIの手法を用いて長期に渡る細胞シートの関節内滞在期間を測定することに成功した．細胞シートはLuc⁺軟骨細胞シート，Luc⁺滑膜細胞シート，両細胞併用シートともに1年以上膝関節内に滞在し続けることをイメージングにより確認できた．イメージングでは右膝以外の発光シグナルを認めず，移植細胞は軟骨細胞，滑膜細胞ともに膝関節内にとどまって長期滞在し，異所への移動(転移)がないことが明らかになった．

細胞シート移植における軟骨の再生効果は，軟骨欠損部が細胞シートの優れた接着性によって覆われることで，関節液中の破壊因子から防御されるとともに，細胞シートからの成長因子を持続的に供給されることで，レシピエント自身の主導的な自己修復が促される[7,10]．そのため細胞シート由来の細胞は移植後2〜3週間で消失すると考えていたが，今回の結果はLuc⁺軟骨細胞シート由来の細胞自身が軟骨欠損部に生着して軟骨再生に寄与する可能性を明らかにした．細胞シートの発光強度は各群移植後，3カ月以降安定して経過するようになり，明らかな増減を認めなかった．ルシフェラーゼ発光強度は細胞数との関連があるが，軟骨細胞，滑膜細胞の細胞環境の差も影響していると考えられる．軟骨細胞と滑膜細胞を併用する効果は，3群とも長期生存を確認したため，1年間の滞在時間においては明らかではなかった．長期に観察されるルシフェラーゼ発光のシグナルはLuc⁺軟骨細胞，Luc⁺滑膜細胞シート由来の間葉系幹細胞の存在の関与も考慮され，今後の研究課題となった．

おわりに

本研究ではBLIの手法を用いて移植した細胞シートの軟骨細胞が関節内で長期滞在することを実証した．細胞シート自身が長期に残存し，軟骨再生に寄与する可能性が新しく示唆された．

謝辞

本研究は，平成21-23年度厚生労働科学研究費補助金再生医療実用化事業「細胞シートによる関節治療を目指した臨床研究」により実施されたものである．

ここに謝意を表する．

文献

1) Contag CH, Ross BD : It's not just about anatomy : *in vivo* bioluminescence imaging as an eyepiece into biology. J Magn Rescon Imaging **16** : 378-87, 2002
2) Contag CH, Spilman S, Benaron D, et al : Visualizing gene expression in living mammals using a bioluminescent reporter. Photochem. Photobiol **66** : 523-531, 1997
3) Contag PR, Olomu IN, Stevenson DK, et al : Bioluminescent indicators in living mammals. Nat Med **4** : 245-247, 1998
4) Hakamata Y, Murakami T, Kobayashi E : "Firefly rats" as an organ/cellular source for long-term in vivo bioluminescent imaging. Transplantation **81** : 1179-1184, 2006
5) Hastings JW : Chemistries and colors of bioluminescent reactions : a review. Gene **173** : 5-11, 1996
6) Kaneshiro N, Sato M, Mochida J, et al : Bioengineered chondrocyte sheets may be potentially useful for the treatment of partial thickness defects of articular cartilage. Biochem Biophys Res Commun **349** : 723-731, 2006
7) Masuoka K, Asazuma T, Nemoto K, et al : Tissue engineering of articular cartilage using an allograft of cultured chondrocytes in a

membrane-sealed atelocollagen honeycomb-shaped scaffold (ACHMS scaffold). J Biomed Mater Res B Appl Biomater **75** : 177-184, 2005
8) Mitani G, Sato M, Mochida J, et al : The properties of bioengineered chondrocyte sheets for cartilage regeneration. BMC Biotechnol **9** : 17, 2009
9) Massoud TF, Gambhir SS : Molecular imaging in living subjects : seeing fundamental biological processes in a new light. Gens Dev **17** : 545-580, 2003
10) Nagai T, Sato M, Mochida J : Optimization of allograft implantation using scaffold-free chondrocyte plates. Tissue Eng Part A **7** : 1225-1235, 2008

リウマチ科，46(4)：406-414，2011

話　題

抗VEGFヒト化モノクローナル抗体投与による関節軟骨修復*

長井敏洋**　佐藤正人**　持田譲治**

Key Words : cartilage repair, bevacizumab

はじめに

関節軟骨は硝子軟骨であり，疎な軟骨細胞と主にII型コラーゲンやプロテオグリカンなどの豊富な細胞外基質から構成される．その基質は含水性に富み約70～80％が水分である．そして血管を有しない関節軟骨は関節液からの拡散により栄養され，適度な粘弾性と非常に少ない摩擦係数を有し，円滑な関節運動が行われている．その関節軟骨の特徴的な構造つまり無血管組織であること，軟骨細胞周囲に密度の高い基質が存在していること，軟骨細胞が高度に分化しており分裂増殖しないことのために，いったん損傷が生じると通常の修復機転が働きにくいため，自己修復能力が著しく乏しい．そのため関節軟骨に損傷や変性が生じると徐々に変形性関節症へと進行する．

変形性関節症をはじめとする運動器疾患は，生命を直接脅かすものではないために，癌や心臓疾患など生命に直接かかわる疾患と比べるとやや軽視されているが，日常生活動作(ADL)を下げるばかりか，生活の質(QOL)の低下も招き，人的社会的損失は計り知れないものがある．2009年度版高齢社会白書によると，わが国の65歳以上の高齢者人口の総人口に占める割合(高齢化率)も22.7％となり，５人に１人が高齢者，10人に１人が75歳以上の人口という未曾有の超高齢社会が到来している．そして健康寿命を縮める原因(要支援となる原因)の第一位が関節疾患20.2％(2007年国民生活基礎調査)となっている．しかしながら，人工関節置換術などの手術適応のある末期の変形性関節症患者を除く初期から中期の患者に対しては漫然と保存的に加療されている現状がある．

関節軟骨修復法

従来から関節軟骨損傷に利用される骨髄刺激法に代表されるdrilling法[1)2)]，microfracture法[3)4)]は軟骨下骨まで欠損を作製し，骨髄から動員される軟骨前駆細胞(修復細胞)を損傷欠損部に供給することにより軟骨修復を期待する方法である．その修復過程は内軟骨性骨化による修復を機転としているため，欠損内部は修復細胞で満たされるが多くの血管侵入を認め，修復組織内部は骨に置換され，表層は主として線維軟骨で修復される[5)6)]．この方法は関節軟骨本来の硝子軟骨の修復でないにもかかわらず，非常に簡便な方法で侵襲も少なく安全性が確立されており，現在最も広く施行されている．しかしながら，線維軟骨による修復の是非に関しては論争中ではあるが，動物実験モデルにおいて線維軟骨による修復は長期経過において関節症性変化をひき起こすと報告されている[7)]．近年では骨軟骨移植法であるmosaic plasty法[8)]が行われるようになり良好な成績が報告され[9)]主流となってきている．この方法は自己の骨軟骨組織を関節非

* Repair of articular cartilage with anti-VEGF antibody bevacizumab.

** Toshihiro NAGAI, M.D., Ph.D., Masato SATO, M.D., Ph.D. & Joji MOCHIDA, M.D., Ph.D.: 東海大学医学部医学科外科学系整形外科学〔〒259-1193 伊勢原市下糟屋143〕; Department of Orthopaedic Surgery, Tokai University School of Medicine, Isehara 259-1193, JAPAN

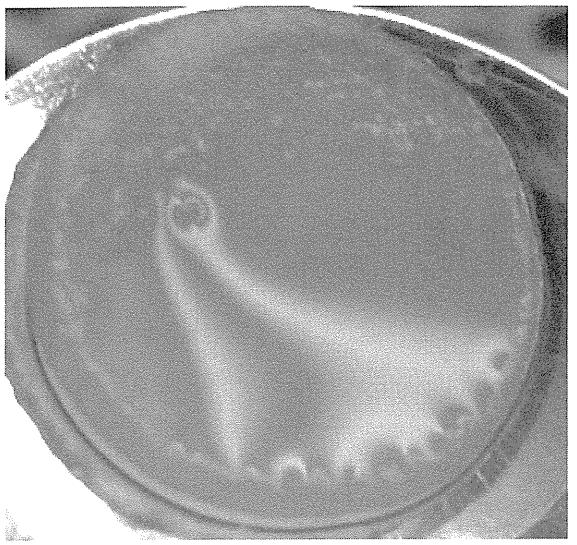

図1　旋回培養法において作成したscaffold free軟骨プレート
直径は10mm.

荷重部から複数個採取し，骨軟骨欠損部にモザイク状に移植する方法である．ただし，採取できる骨軟骨片に限界があること，非荷重部ではあるが正常軟骨に欠損が残ること，移植部位の軟骨形状が再形成されないことなどの問題点が残る．

そこで再生医療による修復を期待してさまざまな治療法が開発・実施されている．黎明期からの細胞移植法[10][11]そして近年では担体(scaffold)やバイオリアクターを用いた組織工学的手法において生体外で構築された軟骨様組織を移植する方法[12][13]が考案され，1990年前半から海外で実施報告され，米国をはじめすでに2万例に近い手術症例の蓄積がある．しかしながら，細胞ならびに組織移植法は，健常部位からの組織採取の問題，移植片の安全性の問題，一定のクオリティーをもった移植片の供給など臨床応用への実現には高いハードルが存在する．また，実用化されても一般施設への普及にはcell processing center所有施設との間で採取組織や移植片の外部輸送が必要となり，その管理体制においても課題が多い．そしてさまざまな担体やバイオリアクターの開発，また担体を使用しない再生組織の構築などを含め，複雑化した製造工程においても真の関節軟骨を作ることが，想像以上に難しいことが明らかになっている．また，その対象疾患は小さな軟骨の外傷性病変にとどまり，再生医療が真に必要とされる変形性関節症の治療には20年近く経過した現在でも至っていない．

本稿ではこれまでに施行したわれわれの動物を用いた基礎的研究の紹介ならびに将来展望について述べる．

骨軟骨欠損モデルの基礎的研究

1. Scaffold free軟骨プレートを用いた動物実験モデル

以前の研究で，われわれは旋回培養法を用いてscaffoldを使用することなく3次元組織工学的軟骨を構築することに成功した[14][15](図1)．日本白色家兎を用いた骨軟骨欠損モデルでの移植動物実験で欠損内部に骨髄から動員される軟骨前駆細胞(自己修復細胞)を満たし，軟骨分化への環境改変誘導因子として表層部のみにscaffold free組織工学的軟骨を移植し良好な長期間の修復効果を得た(図2)．その詳細な修復機序を検討したところ，移植群では移植後早期の骨髄由来の修復細胞で血管新生抑制因子であるコンドロモジュリン-I(ChM-I)の発現を認め，血管新生因子であるvascular endothelial growth factor(VEGF)の発現をほとんど認めなかった．一方，欠損放置群の修復細胞はChM-Iの発現を認めず，VEGFの強発現を認めた(図3)．つまり関節軟骨の特性であるanti-angiogenesis propertyを移植後早期に獲得したことで良好な修復再生効果を発揮することを確認した[16]．

以上の研究により，骨軟骨欠損部に動員される修復細胞のVEGFの生物活性を一時的に阻止することで，細胞移植や組織移植を用いなくとも組織修復の環境改変効果が期待でき，小さな軟骨外傷のみならず変形性関節症の治療にまで踏み込め，移植療法に替わる軟骨再生医療として画期的なものであると仮説を立てた．

2. Bevacizumab(Avastin®)の静脈内投与による動物実験モデル

そこでわれわれはすでに医薬品として使用されている血管新生阻害剤である抗VEGFヒト化モノクローナル抗体bevacizumab(Avastin®)の静脈内投与による関節軟骨全層欠損に対する組織修復の環境改変効果を検討した[17]．

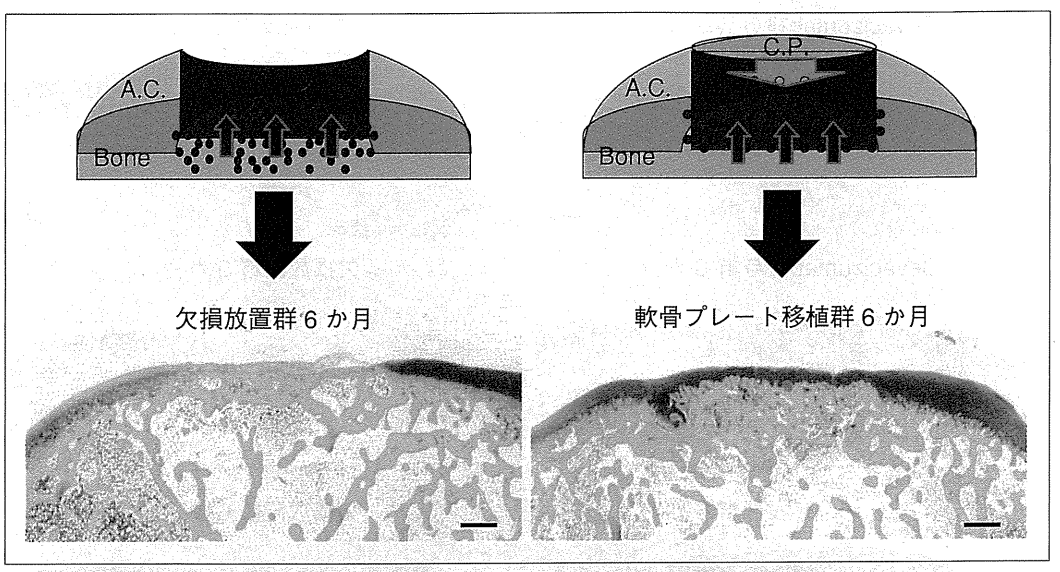

図2　Scaffold free軟骨プレート移植の組織標本（サフラニンO）
上段は骨軟骨欠損モデルにおける欠損放置群と軟骨プレート移植群の修復過程のシェーマ．下段は術後6か月経過した組織標本．染色はサフラニンO染色であり，barは1mm．

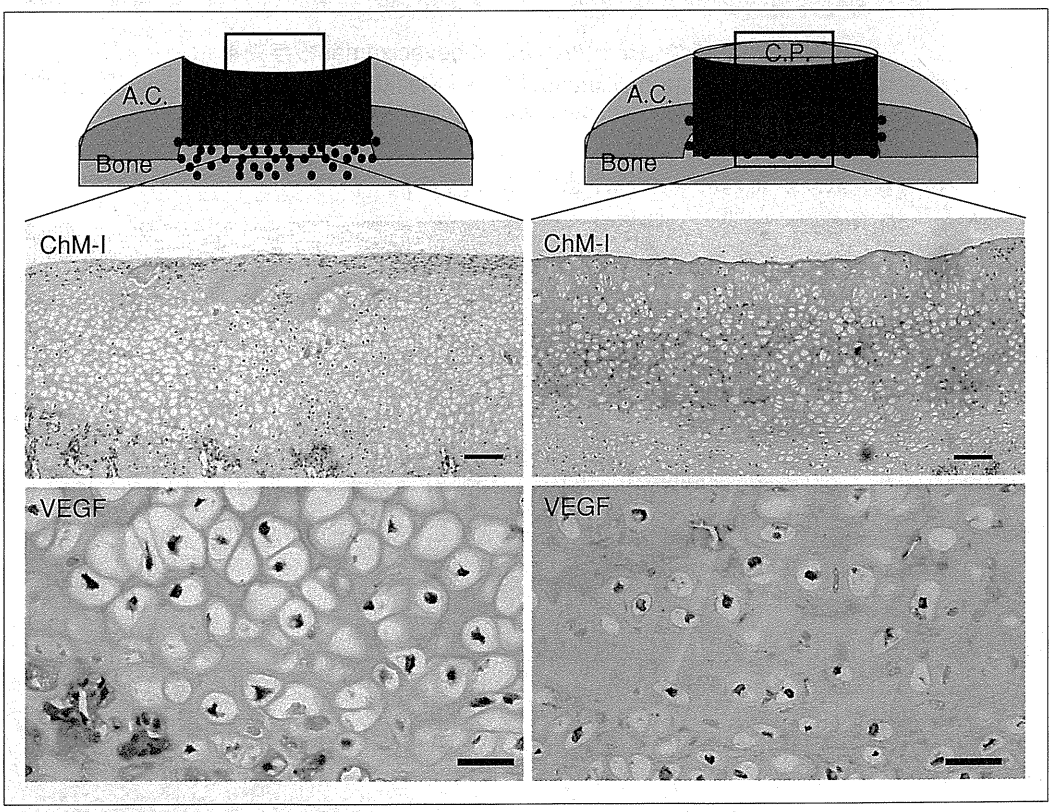

図3　Scaffold free軟骨プレート移植の組織標本（ChM-I，VEGF）
上段は骨軟骨欠損モデルにおける欠損放置群と軟骨プレート移植群の修復過程のシェーマ．中段・下段ともに術後1か月の組織標本．中段はChM-Iの免疫染色でbarは200um．下段はVEGFの免疫染色でbarは50um．

本研究では12週齢の成熟日本白色家兎を使用した．傍膝蓋骨アプローチにおいて関節切開し大腿膝蓋関節に自然修復しない直径5mm深さ3mmの骨軟骨欠損を作製した．Bevacizumab投与群と欠損放置群を作製し，bevacizumab投与群では手術時と術後2週後に1羽につき100mgのbevacizumab

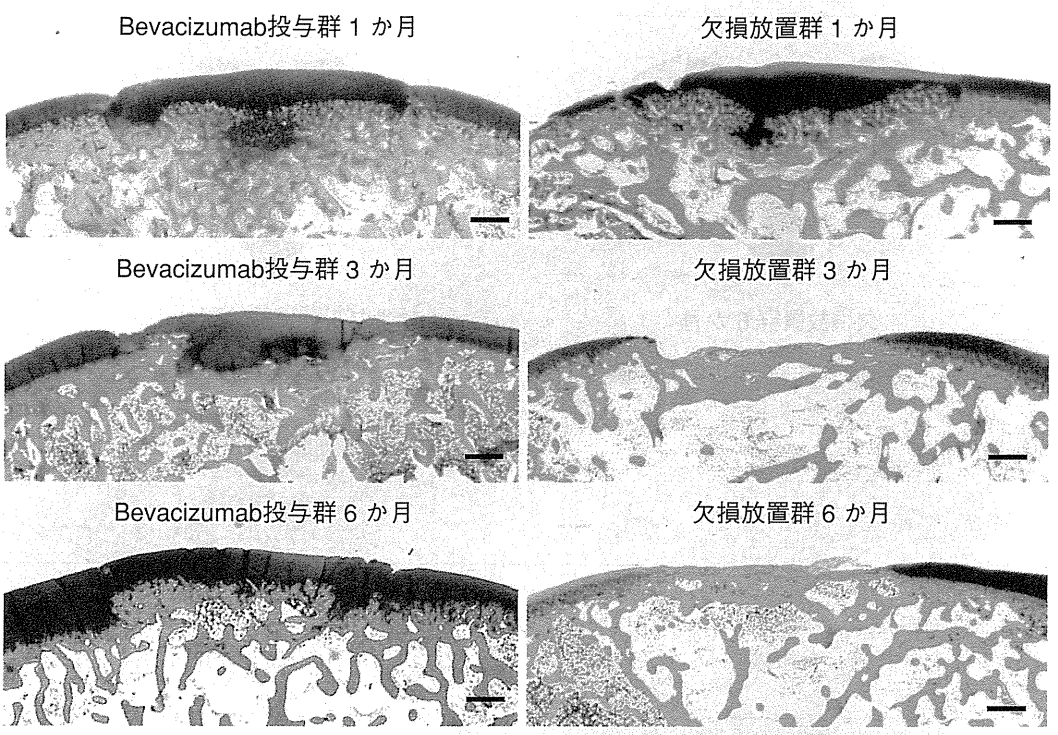

図 4　骨軟骨欠損モデルにおけるbevacizumab投与効果
左側は骨軟骨欠損モデルにおけるbevacizumab投与群で右側は欠損放置群である．上段・中段・下段は順に術後 1・3・6 か月のサフラニン O 染色であり，barは 1 mm.

を静脈内投与した．投与量は家兎に対する抗体感受性から決定した．術後 4 週，12週，24週で犠牲死させ，修復組織の評価をした．

術後 1 か月の欠損放置群の欠損内部はsafranin Oの染色性を認めたが，欠損表層において線維軟骨組織で修復された．一方，bevacizumab投与群の欠損内部はsafranin Oで濃染し，軟骨細胞様に分化した修復細胞で満たされており周囲軟骨との良好なintegrationを認め，欠損部は凸形で修復された．術後 3 か月の欠損放置群は線維性組織での修復を認めた．一方，bevacizumab投与群では，safranin Oの染色性を維持した修復を認め，軟骨下骨の修復も良好であった．修復組織内部の細胞の形態は硝子軟骨様で柱状配列構造を認めていた．術後 6 か月の欠損放置群においても軟骨下骨の露出や線維性組織での修復をうけ，周囲軟骨のsafranin Oの染色性の低下を認めた．一方，bevacizumab投与群では，safranin Oの染色性を維持した修復を認め，平滑な表層を保っていた(図 4)．そこで，術後 6 か月のbevacizumab投与群の修復組織の免疫組織化学的評価をしたところ，硝子軟骨で認められるII型コラーゲンの発現を認め，I 型コラーゲンの発現は認めなかった(図 5)．また，関節軟

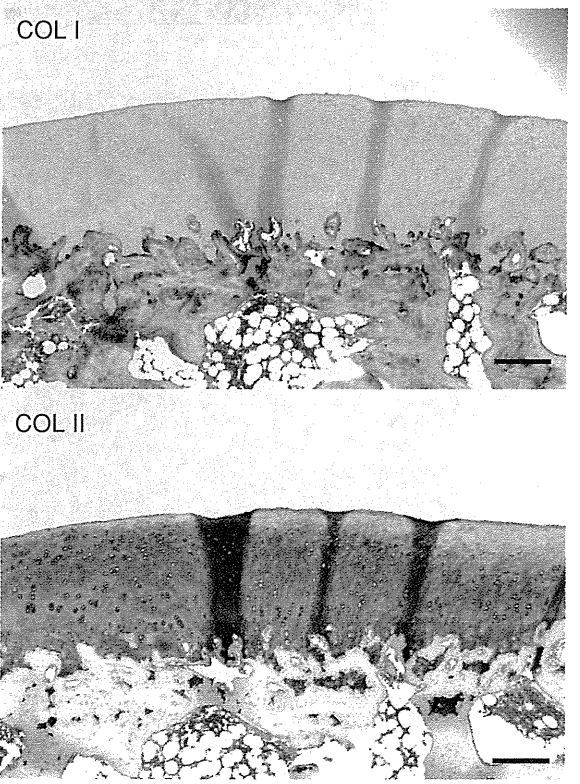

図 5　骨軟骨欠損モデルにおけるbevacizumab投与群における術後 6 か月の組織標本
上段はコラーゲンタイプI・下段はコラーゲンタイプIIの免疫染色でbarは250umである．

骨の潤滑性に関与すると示唆されるsuperficial zone protein(SZP/PRG4)の発現を評価したところ，術後6か月のbevacizumab投与群における修復表層においてもSZPの発現を認めた(図6)．そして軟骨修復効果をInternational Cartilage Repair Society(ICRS)の評価基準(表1)を用いて検討したところ，術後1,3,6か月で欠損放置群と比較してbevacizumab投与群で有意に($P<0.01$)高値を示した(図7)．

欠損放置群とbevacizumab投与群の以上の結果の差違を検討するために，術後1か月における修復細胞の評価をした．欠損放置群ではChM-Iの

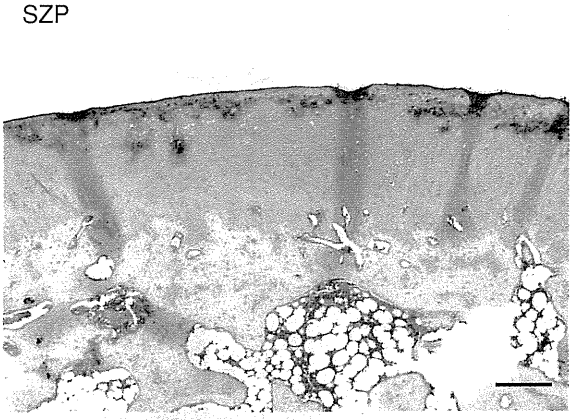

図6　骨軟骨欠損モデルにおけるbevacizumab投与群における術後6か月の組織標本
SZPの免疫染色でbarは250umである．

表1　International Cartilage Repair Society(ICRS)の組織評価基準

Variable	Comment
Ti	Tissue morphology 4＝mostly hyaline cartilage 3＝mostly fibrocartilage 2＝mostly non-cartilage 1＝exclusively non-cartilage
Matx	Matrix staining 1＝none 2＝slight 3＝moderate 4＝strong
Stru	Structural integrity 1＝severe disintegration 2＝cysts or disruption 3＝no organization of chondrocytes 4＝beginning of columnar organization of chondrocytes 5＝normal, similar to healthy mature cartilage
Clus	Chondrocytes clustering in implant 1＝25～100% of cells clustered 2＝＜25% of the cells clustered 3＝no clusters
Tide	Intactness of calcified cartilage layer, formation of tidemark 1＝＜25% of the calcified cartilage layer intact 2＝25～49% of the calcified cartilage layer intact 3＝50～75% of the calcified cartilage layer intact 4＝76～90% of the calcified cartilage layer intact 5＝complete intactness of the calcified cartilage layer
Bform	Subchondral bone formation 1＝no formation 2＝slight 3＝strong
SurfH	Histologic appraisal of surface architecture 1＝severe fibrillation 2＝moderate fibrillation 3＝slight fibrillation or irregularity 4＝normal
FilH	Histologic appraisal defect filling 1＝＜25% 2＝26～50% 3＝51～75% 4＝76～90% 5＝91～110%
Latl	Lateral integration of implanted material 1＝not bonded 2＝bonded at one end/partially both ends 3＝bonded at both sides
Basl	Basal integration of implanted material 1＝＜50% 2＝50～70% 3＝70～90%
InfH	Inflammation 5＝no inflammation 3＝slight inflammation 1＝strong inflammation
Hgtot	Histologic grading system Some of the histologic variables：tissue morphology(Ti), matrix staining(Matx), structural integrity(Stru), cluster formation(Clus), tidemark opening(Tide), bone formation(Bform), histologic surface architecture(SurfH), histologic degree of defect filling(FilH), lateral integration of defect-filling tissue(Latl), basal integration of defect-filling tissue(Basl), and histologic signs of inflammation(InfH) Maximum total：45 points

11～45 pointsでpointが高値であるほど良好な関節軟骨修復となる．

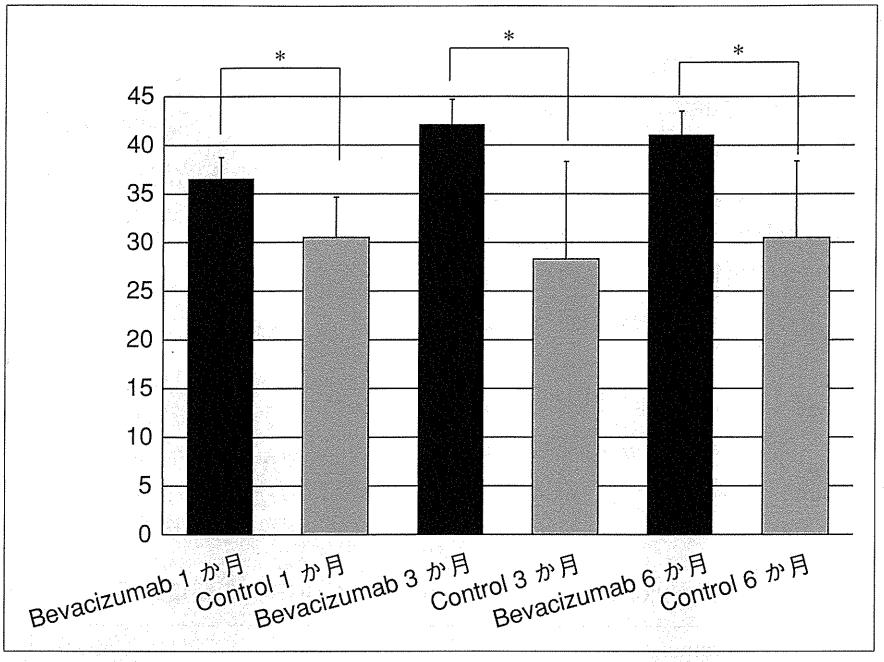

図 7　ICRS組織評価
術後 1・3・6 か月におけるbevacizumab投与群と欠損放置群のICRSの組織評価であり，いずれにおいても有意差($P<0.01$)をもってbevacizumab投与群で高値である．

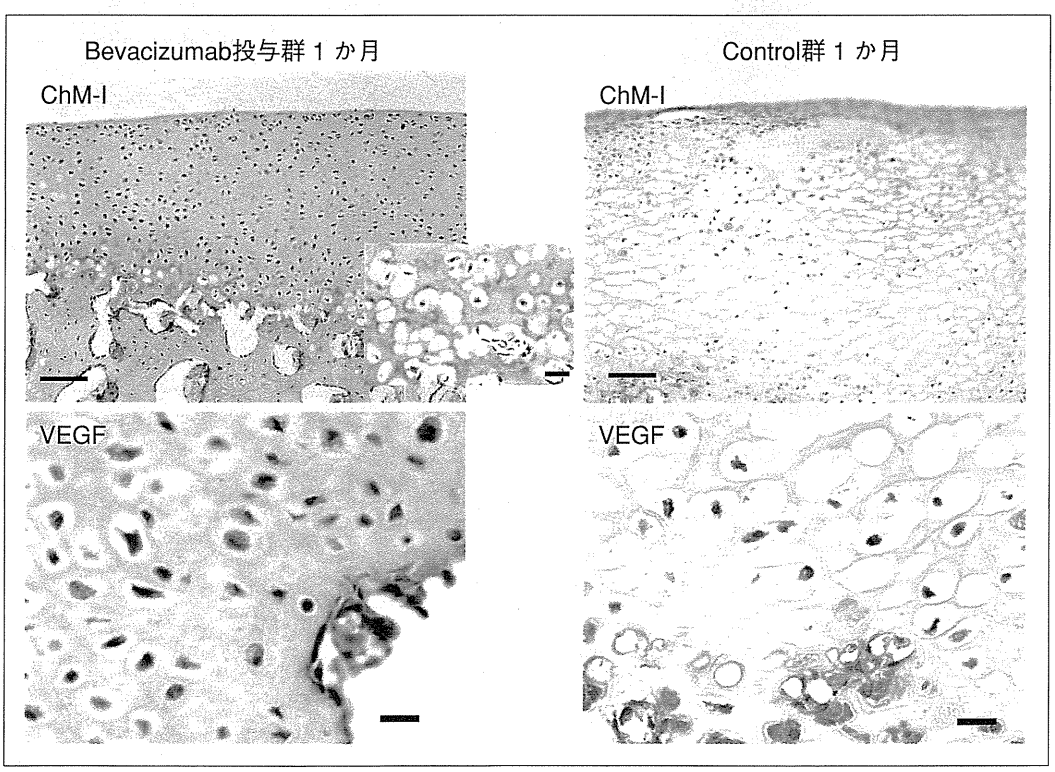

図 8　骨軟骨欠損モデルにおけるbevacizumab投与効果—ChM-I，VEGFの免疫組織化学的染色による評価
左側は骨軟骨欠損モデルにおけるbevacizumab投与群で右側は欠損放置群である．上段・下段ともに術後 1 か月の組織標本．上段はChM-Iの免疫染色でbarは100um，強拡大は50um．下段はVEGFの免疫染色でbarは20um．

発現は認めなかったが，bevacizumab投与群ではChM-Iの発現を一様に認めた．VEGFにおいては，両群の修復細胞で一様に発現を認めた(図8)．

VEGFは，多数の血管形成豊富な固形腫瘍や血液系悪性腫瘍で過剰発現する．したがって，VEGF経路を遮断することは，腫瘍学的な研究の主要焦点になった[18]．近年，悪性腫瘍治療薬として開発された抗VEGFヒト化モノクローナル抗体であるbevacizumabの治療効果が検討されている[19]．Bevacizumabは癌組織から分泌されるVEGFに結合することにより，血管内皮細胞に発現する受容体とVEGFとの結合を阻害し血管新生阻害をひき起こし，癌細胞の増殖を抑制すると報告されている[20][21]．また，bevacizumabは腫瘍のみならず血管新生の阻害治療の可能性が示唆されている[22]．

骨軟骨欠損の修復過程は，内軟骨性骨化による修復を機転としており，欠損内部は骨髄由来の修復細胞で満たされるが周囲からの血管侵入を認め，多くの修復組織の内部は骨に置換される[5][6]．また，肢芽発現の初期において病的な血管新生を介してVEGFは間葉組織の細胞凝集を妨げ[23]，軟骨形成の末期のVEGFの高発現は血管形成を通して内軟骨性骨化につながる[24]と報告されている．さらに，VEGFは関節炎をひき起こす最も重要因子の1つであることが示されており[25]，変形性関節症の軟骨細胞のVEGFの発現は軟骨破壊との関連が示唆されている[26]．また，われわれが以前に施行した組織工学的手法を用いた移植動物実験モデルでは，骨髄由来の修復細胞がanti-angiogenesis propertyを獲得したことで良好な軟骨修復再生効果を導くことを確認している[16]．そこでわれわれは，日本白色家兎を用いた骨軟骨欠損モデルに対して，抗VEGF抗体であるbevacizumabの静脈内投与による組織修復効果を試みた．その結果，術後6か月において良好な軟骨修復過程を確認した．興味深いことは，術後早期におけるbevacizumab投与群の修復組織でChM-Iの発現を獲得したことである．ChM-Iは，無血管組織として関節軟骨を維持し，軟骨損傷に対し再生を促進すると報告されている[27]．本研究でのChM-Iの発現は，軟骨下骨からの血管の侵入を阻止し，関節軟骨の形質発現を獲得するbarrierの働きをしていると考えられる．

しかしながら，VEGFは肢芽発現の際，幹細胞ならびに軟骨細胞のsurvival factorであるとも報告されている[28][29]．本研究では，抗VEGFヒト化モノクローナル抗体であるbevacizumabを骨軟骨欠損部に動員される修復細胞の軟骨分化へのinitiatorとして使用して一時的な使用に留めている．そのため，手術当日と術後2週後の術後早期の投与としており，術後の修復細胞のVEGFの生物活性を完全に阻止しているわけではない．実際，術後1か月の欠損内部で，bevacizumab投与群においてもVEGFの発現を認めていた．また，軟骨下骨からの血管侵入をうける修復細胞の層ではanti-angiogenesis factorであるChM-Iの発現を認めていた．つまり関節軟骨の良好な修復に重要なことは，修復細胞のangiogenesisとanti-angiogenesisのpropertyのbalance，つまり至適なVEGF signalの調整であることが示唆された．

本研究の手法は，関節鏡視下にdrilling法やmicrofracture法を施行し，術後にbevacizumabを静脈内投与するのみであり非常に簡便な方法である．また，既存の軟骨再生医療と併用も可能であるため，さらなる修復効果の向上が期待できる．

将来の展望

現在，われわれは家兎膝前十字靱帯切離モデルを軟骨部分損傷モデル(外傷後変形性関節症モデル)として使用しbevacizumabの投与効果を検討している．変形性関節症において常に混在しながら存在する軟骨部分損傷と骨軟骨損傷の両タイプの軟骨損傷に対してbevacizumab投与による治療効果を示していく予定である．つまり抗VEGFヒト化モノクローナル抗体の静脈内投与のみで，変形性関節症に対する関節軟骨の変性抑制効果を検討することであり，新規の変形性関節症に対する治療法の確立を目指すものである．本薬剤はすでに臨床で使用されており，適応の拡大により，広く多くの施設で治療施行可能となる見込みである．初期から中期の変形性関節症患者を早い時期に根治的に治療することが可能となり，生涯自分自身の関節で過ごせるよう

になれば，人工関節手術を減らせる可能性があり，医療費の削減に大いに貢献するものと考える．そして患者のADLとQOLの向上ひいては国民の健康寿命の延伸に寄与するものである．

文　献

1) Insall J. The Pridie debridement operation for osteoarthritis of the knee. Clin Orthop 1974 ; 101 : 61.
2) Muller B, Kohn D. Indication for and performance of articular cartilage drilling using the Pridie method. Orthopade 1999 ; 28 : 4.
3) Steadman J, Rodkey W, Briggs K, Rodrigo J. The microfracture technique in the management of complete cartilage defects in the knee joint. Orthopade 1999 ; 28 : 26.
4) Mithoefer K, Williams RJ 3rd, Warren RF, et al. Chondral resurfacing of articular cartilage defects in the knee with the microfracture technique : surgical technique. J Bone Joint Surg Am 2006 ; 88 : 294.
5) Shapiro F, Koide S, Glimcher M. Cell origin and differentiation in the repair of full-thickness defects in articular cartilage. J Bone Joint Surg 1993 ; 75A : 532.
6) Caplan AI, Elyaderani M, Mochizuki Y, et al. Principles of cartilage repair and regeneration. Clin Orthop Relat Res 1997 ; 342 : 254.
7) Messner K, Gillquist J. Cartilage repair. A critical review. Acta Orthop Scand 1996 ; 67 : 523.
8) Hangody L, Kish G, Karpati Z, et al. Autogenous osteochondral graft technique for replacing knee cartilage defects in dogs. Orthopedics 1997 ; 5 : 175.
9) Szerb I, Hangody L, Duska Z, Kaposi NP. Mosaicplasty : long-term follow-up. Bull Hosp Jt Dis 2005 ; 63 : 54.
10) Brittberg M, Lindahl A, Nilsson A, et al. Treatment of deep cartilage defects in the knee with autologous chondrocyte transplantation. N Engl J Med 1994 ; 331 : 889.
11) Moseley JB Jr, Anderson AF, Browne JE, et al. Long-term durability of autologous chondrocyte implantation : a multicenter, observational study in US patients. Am J Sports Med 2010 ; 38 : 238.
12) Marcacci M, Berruto M, Brocchetta D, et al. Articular cartilage engineering with Hyalograft C : 3-year clinical results. Clin Orthop Relat Res 2005 ; 435 : 96.
13) Crawford DC, Heveran CM, Cannon WD Jr, et al. An autologous cartilage tissue implant NeoCart for treatment of grade III chondral injury to the distal femur : prospective clinical safety trial at 2 years. Am J Sports Med 2009 ; 37 : 1334.
14) Nagai T, Furukawa KS, Sato M, et al. Characteristics of a scaffold-free articular chondrocyte plate grown in rotational culture. Tissue Eng Part A 2008 ; 14 : 1183.
15) Furukawa KS, Imura K, Tateishi T, Ushida T. Scaffold-free cartilage by rotational culture for tissue engineering. J Biotechnol 2008 ; 133 : 134.
16) Nagai T, Sato M, Furukawa KS, et al. Optimization of allograft implantation using scaffold-free chondrocyte plates. Tissue Eng Part A 2008 ; 14 : 1225.
17) Nagai T, Sato M, Kutsuna T, et al. Intravenous administration of anti-vascular endothelial growth factor humanized monoclonal antibody bevacizumab improves articular cartilage repair. Arthritis Res Ther 2010 ; 12 : R178.
18) Eskens FA. Angiogenesis inhibitors in clinical development. Br J Cancer 2004 ; 90 : 1.
19) Herbert H, Louis F, William N, et al. Bevacizumab plus irinotecan, fluorouracil, and leucovorin for metastatic colorectal cancer. N Engl J Med 2004 ; 350 : 2335.
20) Jain RK. Normalizing tumor vasculature with anti-angiogenic therapy : a new paradigm for combination therapy. Nat Med 2001 ; 7 : 987.
21) Willet CG, Boucher Y, di Tomaso E, et al. Direct evidence the VEGF-specific antibody bevacizumab has antivascular effects in human rectal cancer. Nat Med 2004 ; 10 : 145.
22) Branavan S, Lorraine EH, Ewa MP. Modulation angiogenesis. JAMA 2004 ; 292 : 972.
23) Yin M, Pacifici M. Vascular regression is required for mesenchymal condensation and chondrogenesis in the developing limb. Dev Dyn 2001 ; 222 : 522.

24) Gerber HP, Vu TH, Ryan AM, et al. VEGF couples hypertrophic cartilage remodeling, ossification and angiogenesis during endochondral bone formation. Nat Med 1999 ; 5 : 623.
25) Afuwape AO, Kiriakidis S, Paleolog EM. The role of the angiogenic molecule VEGF in the pathogenesis of rheumatoid arthritis. Histol Histopathology 2002 ; 17 : 961.
26) Enomoto H, Inoki I, Komiya K, et al. Vascular endothelial growth factor isoforms and their receptors are expressed in human osteoarthritic cartilage. Am J Pathol 2003 ; 162 : 171.
27) Hayami T, Funaki H, Yanoeda K, et al. Expression of the cartilage derived antiangiogenic factor chondromodulin-I decreases in the early stage of experiment osteoarthritis. J Rheumatol 2003 ; 30 : 2207.
28) Haigh JJ, Gerber HP, Ferrara N, et al. Conditional inactivation of VEGF-A in areas of collagen2a1 expression results in embryonic lethality in the heterozygous state. Development 2000 ; 127 : 1445.
29) Zelzer E, Mamluk R, Ferrara N, et al. VEGFA is necessary for chondrocyte survival during bone development. Development 2004 ; 131 : 2161.

* * *

European Cells and Materials Vol. 22 2011 (pages 275-290) ISSN 1473-2262

TRANSPLANTATION OF SCAFFOLD-FREE SPHEROIDS COMPOSED OF SYNOVIUM-DERIVED CELLS AND CHONDROCYTES FOR THE TREATMENT OF CARTILAGE DEFECTS OF THE KNEE

J.-I. Lee[1], M. Sato[2,*], H.-W. Kim[1] and J. Mochida[2]

[1]Regenerative Medicine Laboratory, Centre for Stem Cell Research, Department of Biomedical Science and Technology, SMART Institute of Advanced Biomedical Science, Konkuk University, Seoul, Korea
[2]Department of Orthopaedic Surgery, Surgical Science, Tokai University School of Medicine, Kanagawa, Japan

Abstract

Autologous chondrocyte implantation (ACI) is the treatment of choice for osteoarthritis. However, to regenerate articular cartilage using this method, the procedure paradoxically demands that the cell source of the articular chondrocytes (ACs) for *ex vivo* expansion be from the patient's own healthy cartilage, which can result in donor site morbidity. Accordingly, it is essential to develop a substitute for AC. In the present study, we investigated whether synovium-derived cells (SYs) could be used as a partial replacement for ACs in ACI. ACs and SYs from the knees of rabbits were isolated and cultured, and the growth rates of the cells were compared. To manufacture the cellular transplants, we developed a high-density suspension-shaking culture method (HDSS), which circulates the cells in culture media, promoting self-assembly of scaffold-free cellular aggregates. ACs and SYs were mixed in various ratios using HDSS. Injectable cellular transplants were harvested and transplanted into full-thickness osteochondral defects. Simultaneously, histological evaluations were conducted with toluidine blue and safranin O, and immunohistochemistry of collagen type I and II was conducted. Gene expression to evaluate chondrocyte-specific differentiation was also performed. We successfully prepared a large quantity of spheroids (spheroidal cell aggregates) in a short time using mixed ACs and SYs, for all cellular composition ratios. Our data showed that the minimal therapeutic unit for the transplants contributed to *in situ* regeneration of cartilage. In summary, SYs can be used as a replacement for ACs in clinical cases of ACI in patients with broad areas of osteoarthritic lesions.

Keywords: Articular cartilage regeneration, injectable scaffold-free spheroids, high density suspension shaking culture method, synovium-derived cells, chondrocytes.

*Address for correspondence:
Masato Sato
Department of Orthopaedic Surgery, Surgical Science,
Tokai University School of Medicine,
143 Shimokasuya, Isehara, Kanagawa, 259-1193 Japan
Telephone Number: +81-463-93-1121 (ext 2320)
FAX Number: + 81-463-96-4404
E-mail: sato-m@is.icc.u-tokai.ac.jp

Introduction

Adult articular cartilage has a limited capacity for self-repair after either degeneration or injury occurs and is therefore unlikely to be restored to normal once it has been damaged.

Autologous chondrocyte implantation (ACI), first reported by Brittberg group (Brittberg *et al.*, 1994), has been used clinically. Promising results for transplantation of cultured autologous cartilage cells have been reported, and various articular cartilage regeneration techniques have been clinically applied, including the use of scaffolds such as atelocollagen (Ochi *et al.*, 2002) and cell transplantation therapy with articular chondrocytes, synovium-derived cells (Shimomura *et al.*, 2010), and bone marrow-derived mesenchymal stem cells (Wakitani *et al.*, 2002). In addition, tissue-engineered cartilage with varying scaffold materials (Buckwalter and Mankin, 1998; Freed *et al.*, 1994; Ochi *et al.*, 2001; Darling and Athanasiou, 2003) or without scaffolds (Brehm *et al.*, 2006; Nagai *et al.*, 2008a; Nagai *et al.*, 2008b; Mitani *et al.*, 2009) have been developed and introduced.

While clinical results have shown that ACI can be beneficial, problems remain, such as periosteal hypertrophy, limits on the size of lesions that can be treated due to associated donor site morbidity, ability to treat only a predetermined defect area, alterations in the chondrogenic phenotype associated with *in vitro* expansion of the cells, and lengthened *ex vivo* culturing time for preparing a large amount of articular chondrocytes (ACs). In addition, due to alterations and degenerative changes in cartilage accompanying aging, the availability of such cells may be limited in elderly patients (Nehrer *et al.*, 2006; Iwasa *et al.*, 2009).

To overcome these issues, therapies using stem cells have been studied to facilitate tissue repair. Recently, research has focused on synovium-derived cells (SYs), whose high proliferative potency does not change with age, associated with mesenchymal stem cells (MSCs) that have the capacity to differentiate into chondrocytes. SYs of MSCs have the capability to proliferate and differentiate into a variety of connective tissue cells (De Bari *et al.*, 2001). ACs from aged patients show limited proliferation *in vitro*; in contrast, MSCs are an attractive cell source for cartilage regenerative medicine because they can be harvested in a minimally invasive manner, are easily isolated and expanded, and have multipotentiality that includes chondrogenesis (Prockop, 1997; Pittenger *et al.*, 1999; Sekiya *et al.*, 2002; Sakaguchi *et al.*, 2005). In addition, synovial MSCs are especially promising due to

their high proliferative capacity and chondrogenic potential (Sakaguchi *et al.*, 2005; Mochizuki *et al.*, 2006; Yoshimura *et al.*, 2007; Nagase *et al.*, 2008; Nimura *et al.*, 2008).

As disadvantages of pure cell suspension delivery were identified in several previous studies, artificial scaffolds have been adopted to deliver cells into cartilage-defect sites and to reinforce the mechanical stability of three-dimensional (3D) tissue-engineered chondral grafts. An ideal scaffold would encourage the development of the extracellular matrix (ECM). Although a few scaffolds have been applied successfully to cartilage regeneration (Masuoka *et al.*, 2005), challenges remain regarding biocompatibility and cellular viability, including cell attachment, distribution, and proliferation (Mitani *et al.*, 2009). Biological or synthetic materials can cause immunological problems such as acute rejection, foreign body reaction, or fibroblastic overgrowth (Anderson *et al.*, 2008; Badylak and Gilbert, 2008), which have an impact on the therapeutic effect.

Accordingly, we have developed 3D, scaffold-free, tissue-engineered cartilaginous tissues (Nagai *et al.*, 2008a; Mitani *et al.*, 2009) from chondrocytes and transplanted these tissues into the region of osteochondral defects as an initiator of cartilage differentiation in reparative cells (Kaneshiro *et al.*, 2006; Nagai *et al.*, 2008b); we achieved good long-term restoration results. However, the overall process of these methods requires a comparatively long period (more than 4 weeks), as reported previously for studies of ACI (Brittberg *et al.*, 1994; Freed *et al.*, 1994; Buckwalter and Mankin, 1998; Ochi *et al.*, 2001; Ochi *et al.*, 2002; Wakitani *et al.*, 2002; Darling and Athanasiou, 2003; Brehm *et al.*, 2006; Shimomura *et al.*, 2010). Therefore, a shortened process for the preparation of ACI was accomplished using a high-density suspension-shaking (HDSS) culture method, which allows an equivalent amount of mass transfer to be achieved more quickly, thereby increasing the feasibility of this ACI using a new scaffold-free transplantation system. Conversely, as is well known, pellet culture is a representative 3D culture technique. A pellet culture system that allows cell–cell interactions, analogous to those that occur in pre-cartilage condensation during embryonic development, has been reported as a way to prevent and reverse the phenotypic modulations of chondrogenesis *in vitro*. Because this system forms only one aggregate, this aggregate cannot be used to produce tissue-engineered cartilage (Furukawa *et al.*, 2003).

The purpose of this study was to evaluate the feasibility of a new method for scaffold-free spheroids (spheroidal cell aggregates) using an HDSS method originally devised to manufacture structures comprising two types of cells, and to investigate whether ACs and SYs form transplantable spheroids for cartilage regeneration in rabbits. To investigate the effects of implantation, we conducted animal experiments using these scaffold-free transplants. The recovered spheroids, which were constructed using different mixing ratios, were analysed histopathologically and morphologically, and a gene expression analysis was performed to test the cartilaginous phenotype. The results revealed that our HDSS culture system shortened the preparation time by half (less than 2 weeks) and produced a considerable amount of spheroids for ACI.

Materials and Methods

Animal experiments were approved and carried out following the Guidelines of Tokai University on Animal Use.

Primary cultures of articular chondrocytes and synovium-derived cells

With the rabbits under isoflurane (Forane®; Abbott Japan, Tokyo, Japan) anaesthesia (induction 4 %, maintenance 2.0 % under 30 % oxygen and 70 % nitrous oxide), specimens of articular cartilage and synovium with subsynovial tissue were harvested from the knee joints of 4-week-old male Japanese white rabbits weighing approximately 1 kg. The cartilage and synovial tissues were stored in basal medium (BM) containing Dulbecco's modified Eagle's medium/ F12 (DMEM/F12; Gibco/ Invitrogen, Carlsbad, CA, USA) supplemented with 10 % heat-inactivated foetal bovine serum (FBS; Gibco/Invitrogen), 50 μg/mL ascorbic acid (Nissin Pharmaceutical Co, Yamagata, Japan), and 1 % antibiotic-antimycotic mixture (ABAM; 10,000 U/mL penicillin G, 10,000 μg/mL streptomycin sulphate, and 25 μg/mL amphotericin B as Fungizone; Gibco/Invitrogen) until required for the next step. The samples were cut using scissors with curved blades on a watch glass (120 mm diameter; Toshinriko Co., Tokyo, Japan). Thereafter, the finely chopped specimens were digested for 3-4 h in BM containing 0.5 % collagenase (collagenase class I; Worthington Biochemical, Lakewood, NJ, USA).

The digested cell suspensions were passed through a cell strainer (BD Falcon™; BD Bioscience, Bedford, MA, USA) with a pore size of 70 μm, and the isolated cells were rinsed twice with chilled Dulbecco's phosphate-buffered saline (PBS; Dainippon Pharmaceutical, Osaka, Japan). The isolated primary cells were counted on a Burker-Turk haematocytometer (Erma, Tokyo, Japan) with trypan blue staining. The ACs and SYs were then each seeded into 500 cm^2 dishes (245 × 245 mm; Corning, Corning, NY, USA) at a density of 20,000 cells/cm^2 and cultured in BM with 10 % FBS at 37 °C under an atmosphere of 5 % humidified CO_2 and 95 % air according to previously reported methods for ACs of (Mitani *et al.*, 2009) and for SYs of (Koga *et al.*, 2007). The culture medium was changed twice a week. The cells were cultured until 90 % confluence as passage 0. At subconfluence, the seeded cells were expanded by sequential passages in monolayer cultures in BM with 10 % FBS. Each passage of AC and SY cells was detached using 0.05 % trypsin/ethylene-diaminetetraacetic acid (EDTA; Gibco/Invitrogen) for 20-30 min at 37 °C. The cells were centrifuged at 200 *g* for 5 min. The washed pellet was resuspended in medium and the passages were subsequently reseeded under the same conditions described above. The cells were trypsinised and further expanded for passage.

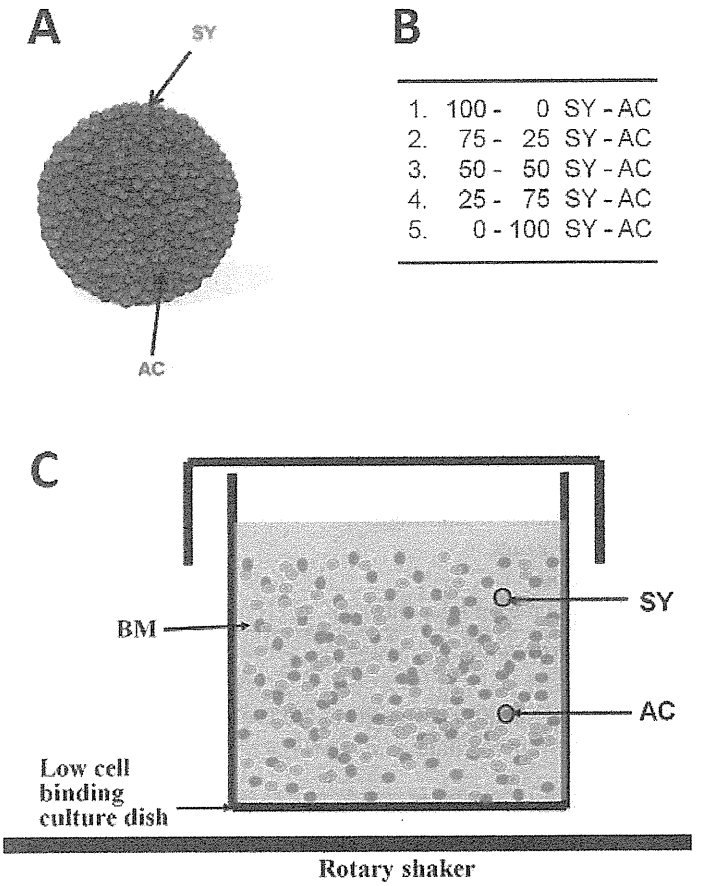

Fig. 1. Construction of scaffold-free spheroids. (**A**) Schematic illustration of the manufacture of scaffold-free spheroids. (**B**) Recovered ACs and SYs were mixed in various ratios and subjected to either morphological evaluation or gene expression analysis. In addition to the *in vitro* analyses, we selected the optimum ratio of ACs and SYs (2. 75:25 SY:AC) for *in vivo* implantation. (**C**) Schematic illustration of the high-density suspension-shaking culture method (HDSS). To fabricate the spheroids, a total of 1.0×10^7 cells/5 mL medium was plated on each low cell-binding culture dish and the shaking culture was maintained at 37 °C under 5 % CO_2. A rotary shaker was used for circular movement at 70 rpm. BM: basal medium, SYs: synovium-derived cells, ACs: articular chondrocytes.

Proliferation potential

To compare the proliferative potency of the ACs and SYs, we defined and calculated the passaging growth rate (PGR). The PGR for each culture dish was calculated per culture day using the following formula: PGR = (recovered cell numbers for a given passage/seeded number of cells for the passage)/culturing days until the next passage.

Fluorescent dye staining

To evaluate the morphology and the distribution within the spheroids with mixed ACs and SYs, isolated ACs and SYs were labelled with PKH-26 (Red Fluorescent Cell Linker Kit for General Cell Membrane Labelling; Sigma-Aldrich, St. Louis, MO, USA) and PKH-67 (Green Fluorescent Cell Linker Kit for General Cell Membrane Labelling; Sigma-Aldrich), respectively, prior to spheroid culture. The PKH fluorescent cell linker kits, which are stably incorporated and retained in the plasma membrane, are nonradioactive and lipophilic substances with no known cellular toxicity, having a fluorescent half-life of >100 days in erythrocytes (according to the manufacturer's package insert) (Samlowski *et al.*, 1991). Labelling was performed according to the manufacturer's instructions, i.e., reacting 2.0×10^7 cells with PKH-26 or PKH-67 in F12/DMEM without serum at 25 °C for min.

Manufacture of the scaffold-free spheroids

We fabricated the mixed cellular scaffold-free constructs using HDSS modified from the original method (Fig. 1A) (Lee, 2007). Briefly, ACs and SYs were harvested and counted on a Burker-Turk haematocytometer with trypan blue staining, and subsequently resuspended in BM with 10 % FBS. Recovered ACs and SYs were mixed at various ratios: 75:25, 50:50 and 25:75. ACs alone (100) and SYs alone (100) were also prepared for analysis (Fig. 1B). Upon mixing, 1.0×10^7 cells/5 mL medium were plated in a low cell-binding culture dish (60 mm Hydrocell™; Cellseed Co., Tokyo, Japan) and maintained in the shaking culture at 37 °C under 5 % CO_2. A rotary shaker (Double Shaker NR-3; Taitec, Koshigaya, Japan) was used to maintain

Table 1. Grading Scale for Gross Appearance. This table was extracted from Cook *et al.* (2003).

Description	Points
Intraarticular adhesions	
None	2
Minimal/fine loose fibrous tissue	1
Major/dense fibrous tissue	0
Restoration of articular surface	
Complete restoration	2
Partial restoration	1
No restoration	0
Erosion of cartilage	
None	2
Defect site/site border	1
Defect site and adjacent normal cartilage	0
Appearance of cartilage	
Translucent	2
Opaque	1
Discolored or irregular	0
Maximum total	***8***

Table 2. Histological Grading Scale for Defect Cartilage. This table was extracted from Wakitani *et al.* (1994).

Category	Points
Cell Morphology	
Hyaline cartilage	0
Mostly hyaline cartilage	1
Mostly fibrocartilage	2
Mostly noncartilage	3
Noncartilage only	4
Matrix Staining (Metachromasia)	
Normal (compared with host adjacent cartilage)	0
Slightly reduced	1
Markedly reduced	2
No metachromatic stain	3
Surface Regularity	
Smooth (3/4)	0
Moderate (1/2-3/4)	1
Irregular (1/4-1/2)	2
Severely irregular (1/4)	3
Thickness of Cartilage	
2/3	0
1/3-2/3	1
1/3	2
Integration of Donor with Host Adjacent Cartilage	
Both edges integrated	0
One edge integrated	1
Neither edge integrated	2
Maximum Total	***14***

circular movement at a speed of 70 rpm (Fig. 1C). After 2-3 days of culture, the spheroidal cell aggregates were collected and divided for *in vivo* implantation and *in vitro* analysis including histology, immunohistochemistry, and gene expression.

In vivo transplantation

Cartilage and synovium tissues were harvested from two different donor rabbits (4 week old male Japanese white rabbits weighing approximately 1 kg) according to time (8 or 16 weeks) after the transplantation of spheroids. These tissues were treated to obtain each of the primary cell lines. Twelve Japanese white rabbits (females, 16-18 weeks old, weighing ~3 kg) were used for transplantation in this study. The rabbits were anaesthetised with isoflurane (induction 4 %, maintenance 2.0 % under 30 % oxygen and 70 % nitrous oxide). After a medial parapatellar incision to both legs, each patella was dislocated laterally, and a

superficial osteochondral defect (5 mm in diameter and 3 mm deep) was created on the patellar groove of the femur in both legs using a drill and a biopsy punch (Kai Industries, Seki City, Japan). The bottom of the subchondral bone was shaved to a plane using a biopsy punch until bleeding was seen from the marrow, as described previously (Nagai *et al.*, 2008b). Rabbits were classified into two recipient groups: an injectable spheroid-implanted group, in which the scaffold-free transplants were allografted into the defect that was created, and a non-transplanted control group. Before allograft transplantation, spheroids were collected from a culture dish through micropipette tips and were then delivered into the defect using micropipette aspiration. The defect was filled with scaffold-free spheroids, which were processed and prepared with 1.0×10^7 cells in 200 μL of medium, and was held stationary for 15 min without any additional fixation. The joint capsule and soft tissue were then closed in routine fashion. After recovery from the surgery, all animals were allowed to walk freely in their cages without splints.

Morphologic evaluation *in vitro* and *in vivo*

At the end of the study periods, the rabbits were euthanised with a lethal dose of 120 mg/kg sodium pentobarbital (Abbott Laboratories, Abbott Park, IL, USA).

Macroscopic evaluations of the transplanted areas were conducted at 8 or 16 weeks postoperatively. The six femoral knee joints per group (n = 3) were evaluated immediately after the rabbits were euthanised. The distal parts of the femur were harvested and observed. The cartilage defects were examined and scored macroscopically for the presence of intraarticular adhesions, completeness of surface restoration, signs of cartilage erosion, and the overall appearance of each defect, including smoothness, colour, and integrity, according to a gross appearance grading scale consisting of four categories with a total score ranging from 0-8 points (best score, 8; worst score, 0), as described by Cook *et al.* (2003) (Table 1).

After macroscopic evaluation, the distal part of the femur was excised and fixed in 4 % paraformaldehyde for 7 days. Each specimen was decalcified in a solution of 10 % EDTA in distilled water (pH 7.4) for 2-3 weeks and then embedded in paraffin wax and sectioned perpendicularly (4 μm sections) through the centre of the defect. The sections were then deparaffinised according to standard procedures.

Spheroid samples were washed with PBS, then immersed in PBS containing 15 % and 20 % sucrose and immediately frozen, embedded in OCT compound (Sakura Finetechnical, Tokyo, Japan), and sectioned at a thickness of 4 μm.

After pretreatment of tissue and spheroid specimens, each section was stained with toluidine blue (for detection of proteoglycans) and safranin O (for detection of glycosaminoglycans) for histological evaluation. Immunohistochemistry was conducted as described previously (Nagai *et al.*, 2008b). In brief, the sections were treated with 0.005 % proteinase (Type XXIV; Sigma-Aldrich) for 30 min at 37 °C for antigen retrieval. For types I and II collagen, a primary mouse monoclonal antibody (Daiichi Fine Chemical Co., Toyama, Japan) diluted 1:200 in PBS + 1 % bovine serum albumin (BSA; Sigma-Aldrich) (final concentration 2.5 mg/mL) was placed on the section overnight at 48 °C. The remaining sections were incubated with PBS instead of specific primary antibodies and stained as negative controls. The slides were washed with PBS after incubation for 1 h at room temperature with biotin-conjugated goat anti-mouse secondary antibody (Cortex Biochem, San Leandro, CA, USA) for type I collagen and type II collagen. The slides were then treated with horseradish peroxidase-labelled streptavidin (Dako, Glostrup, Denmark) for 1 h and were then soaked in a 0.05 % solution of diaminobenzidine in Tris-HCl buffer (pH 7.6) containing 0.005 % hydrogen peroxide. The slides were counterstained with Mayer's haematoxylin and evaluated microscopically.

The sections were scored according to a histological grading scale. We used Wakitani's Scale consisting of 5 categories (cell morphology, matrix staining, surface regularity, cartilage thickness, and integration of donor with host) with a total score ranging from 0 to 14 points (best score, 0; worst score, 14) as described by Wakitani *et al.* (1994) (Table 2). The total scores were compared between groups.

Morphologic evaluation of the spheroids was performed using phase-contrast microscopy and fluorescence microscopy (AX70; Olympus, Tokyo, Japan). To evaluate the location and distribution of cells in the spheroid structures composed of ACs and SYs, the spheroids were analysed using the lambda stack function of the confocal microscope (LSM 510 Meta; Zeiss, Oberkochen, Germany).

The threshold for PKH67 and PKH26 was set by evaluating the highest exposure at which the unlabeled ACs or SYs showed no autofluorescence.

RNA extraction and reverse transcription-polymerase chain reaction

Intact total RNA was isolated and extracted from spheroids with various cellular ratios (SY:AC: 100:0, 75:25, 50:50, 25:75, 0:100) both at the beginning (0 h) and on day 3 of HDSS using the SV Total RNA Isolation System (Promega, Madison, WI, USA), which included DNase digestion and spin column purification. 18S ribosomal RNA was used as an internal standard (Applied Biosystems, Foster City, CA, USA). The primers for rabbit collagen type I and II were obtained from Invitrogen and designed using Primer Express 3.0 (Applied Biosystems), based on sequences from the GenBank database ([Genbank: D49399 and D83228] respectively). For rabbit collagen type I the primers used were GCCTCGCTCACCACCTTCT (forward) and CAATCTGGTTGTTCAGAGACTTCAG (reverse). For rabbit collagen type II the primers used were GCAGCACGTGTGGTTTGG (forward) and CAGGCTGCTGTC TCCATAGCT (reverse). For each sample, 2 μg of total RNA was reverse transcribed into cDNA using Multi- Scribe Reverse Transcriptase (Applied Biosystems) and Random Hexamers (Applied Biosystems). For PCR 5 μL of cDNA template was amplified in a 25 μL reaction volume of GeneAmp PCR buffer (Applied Biosystems), containing 5.5 mM $MgCl_2$, 200 μM of each dNTP, 0.5 μM of appropriate primer pairs and 1 unit of AmpliTaq Gold DNA polymerase (Applied Biosystems).

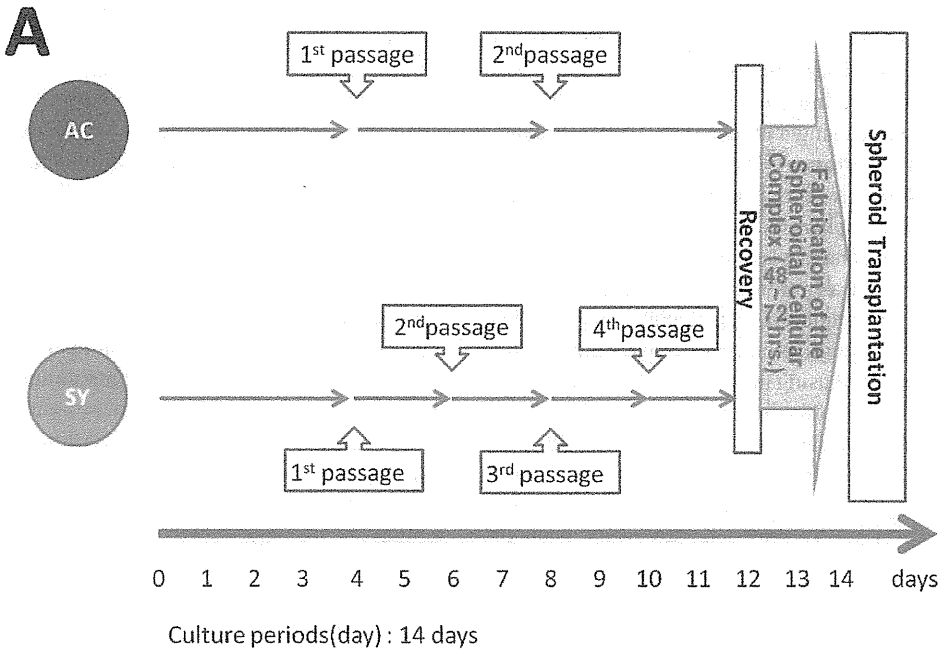

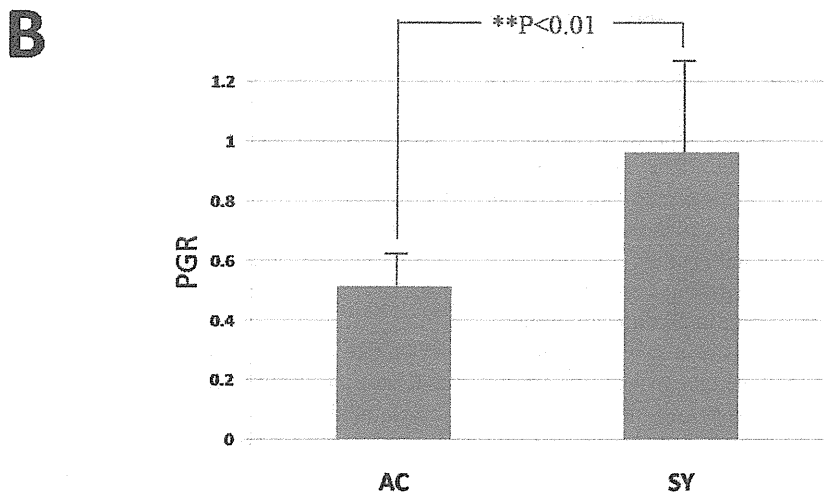

Fig. 2. HDSS schedule and passaging growth rate. **(A)** Schedule for manufacturing the SY-AC spheroids. During 11-12 days of continuous culture passaging, we performed three passages for ACs and five passages for SYs. The third AC passage and the fifth SY passage were utilised to fabricate the scaffold-free spheroids. After 2-3 days of HDSS, the cellular aggregates were considered stable enough to be handled. **(B)** Comparison of proliferative potency between the SYs and ACs. The PGR for the SYs was significantly higher than that of the ACs. PGR: passaging growth rate.

The reaction mixture was kept at 95 °C for 10 min for a 'hot-start', followed by PCR of 40 cycles. Each cycle included denaturation at 95 °C for 15 s, followed by annealing and extension at 61 °C for 1 min. A total of 10 μL of each PCR product was applied to 3 % NuSieve® 3:1 agarose gel (Lonza Rockland, Rockland, ME, USA) for electrophoresis. Resolved bands on the gels were visualised with 0.5 mg/L ethidium bromide on a densitograph system (ATTO Biotechnologies, Tokyo, Japan).

Statistical analysis

Data are presented as means ± standard deviations (SD) of measurements from 6 independent experiments. Groups were compared by analysis of variance (ANOVA). Student's *t*-test was used to determine significant differences. Values of $p < 0.05$ were considered the minimum level of statistical significance.

Results

Primary cultures of chondrocytes and synovium-derived cells from articular cartilage

Using the methods described above, the recovered numbers of AC and SY cells from a single knee joint were 850.9×10^4 $\pm24.2\times10^4$ and 593.3×10^4 $\pm47.0\times10^4$, respectively. During

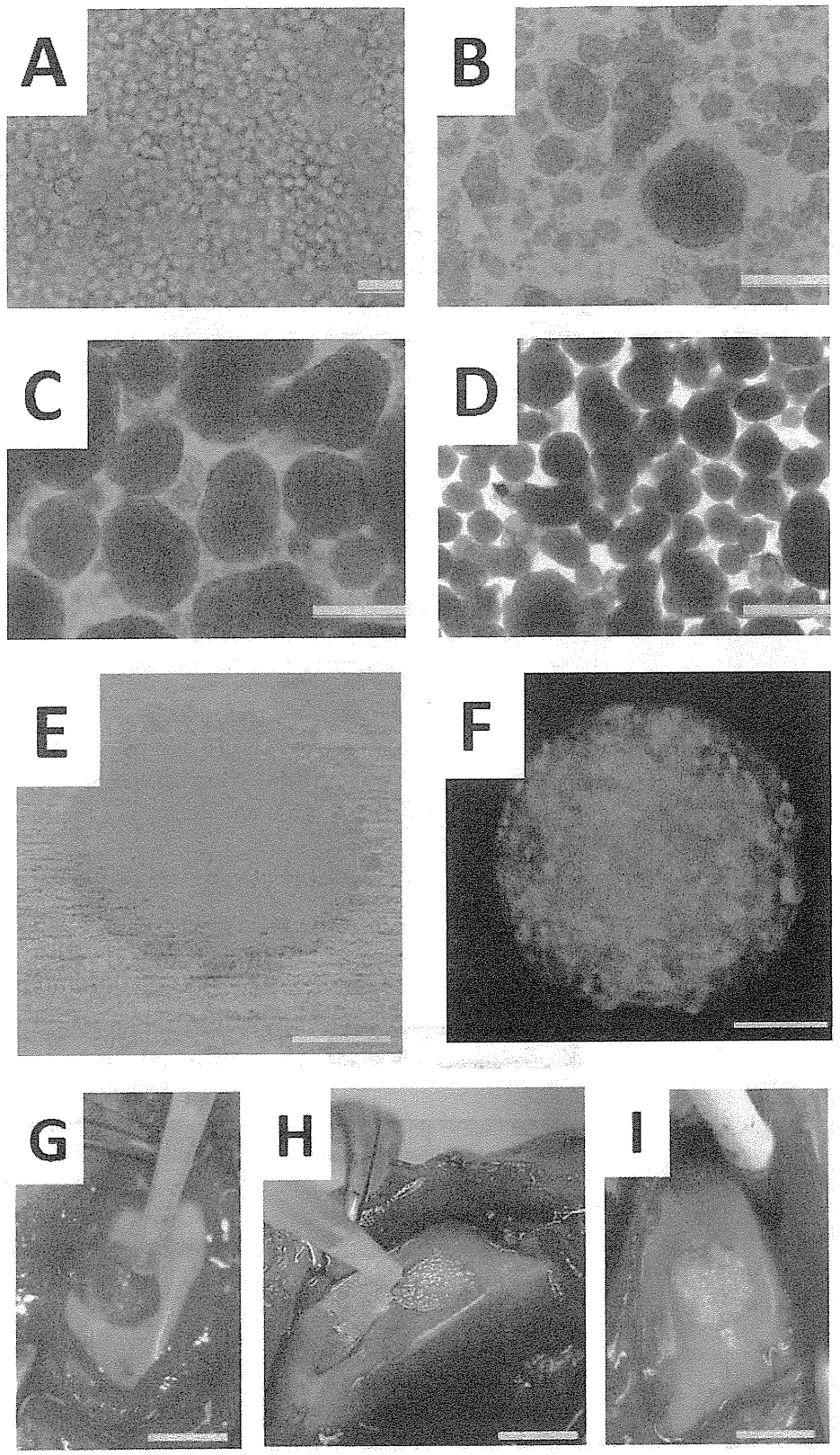

Fig. 3. Implantation of injectable spheroids. Changes in the appearance of representative cellular aggregates (75:25 SY:AC) with HDSS over time compared to other SY:AC ratios under a phase contrast micrograph at (**A**) 0 h, bar = 50 μm; (**B**) 12 h, bar = 200 μm; (**C**) 24 h, bar = 200 μm; and (**D**) 36 h, bar = 500 μm. (**E**) Macroscopic appearance of the spheroids (75:25 SY:AC) after HDSS. Bar = 5 mm. (**F**) A representative spheroid (50:50 SY:AC) under confocal microscopy. Bar = 100 μm. (**G**) The spheroids were collected and delivered to the osteochondral defect site using micropipette aspiration through a micropipette tip. (**H**) The defect was filled with scaffold-free spheroids (75-25 SY:AC) in 200 μL medium and (**I**) left stationary for 15 min without any additional fixation. Bar = 5 mm.

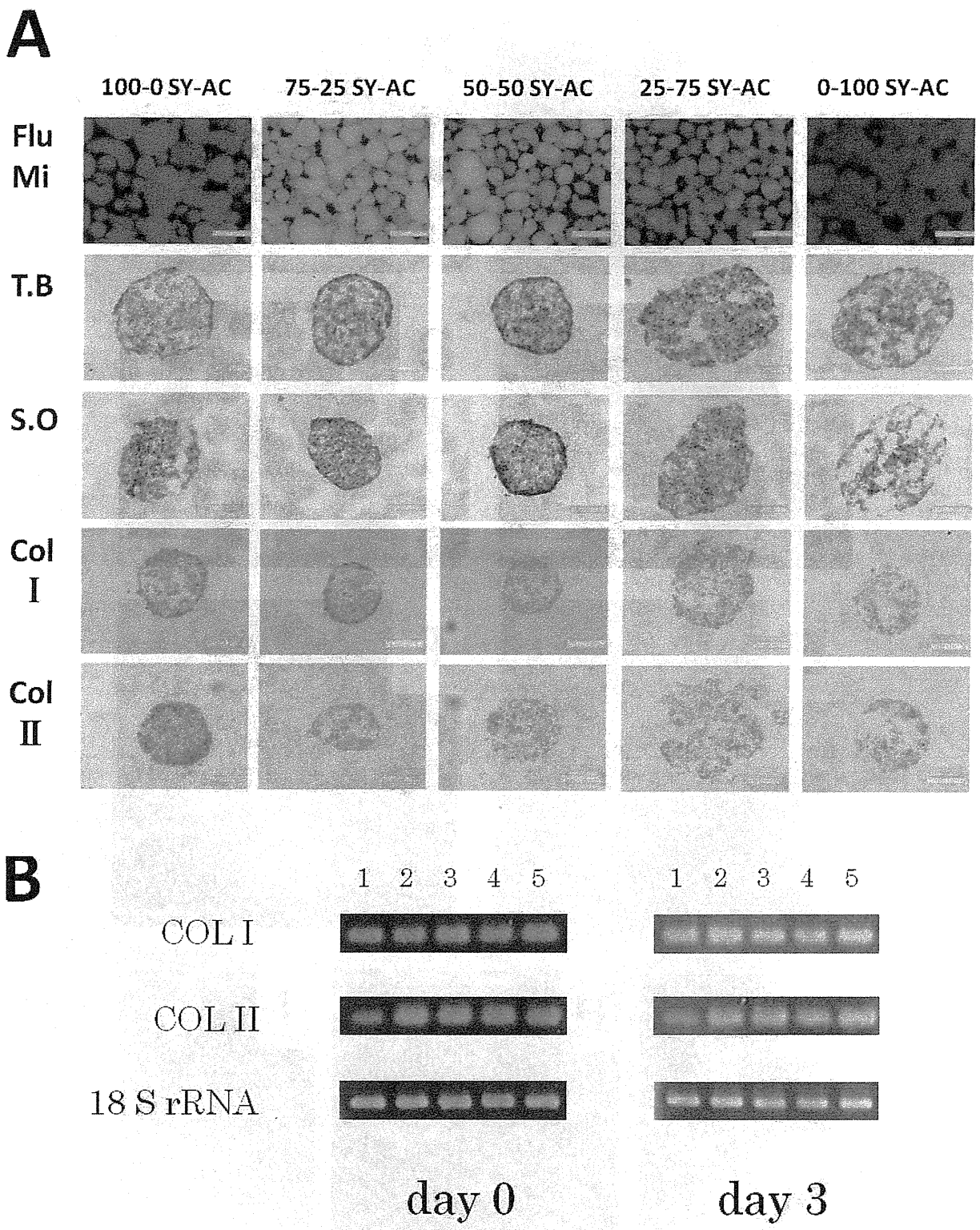

Fig. 4. Morphological analysis and RT-PCR results of spheroids. (**A**) Morphologic appearance under fluorescence microscopy (Flu Mi, Bar = 500 μm) of the completed structure of each spheroid type after a 36 h culture. For histological analysis, spheroids with different ratios of SY:AC subjected to 3 days of HDSS were evaluated with toluidine blue (TB) and safranin O (SO) staining. There were no prominent differences in the staining patterns among the cell composition ratios for any structures. None of the spheroids showed a normal cartilage phenotype regardless of cellular composition. For all spheroid compositions, the ECM was sparsely and irregularly stained with SO and TB, suggesting a small amount of glycosaminoglycans and proteoglycans, and was also positive for type I and type II collagen. Bar = 100 μm. (**B**) RT-PCR analysis showed that both type I and type II collagen was expressed in each spheroid, regardless of cellular composition.

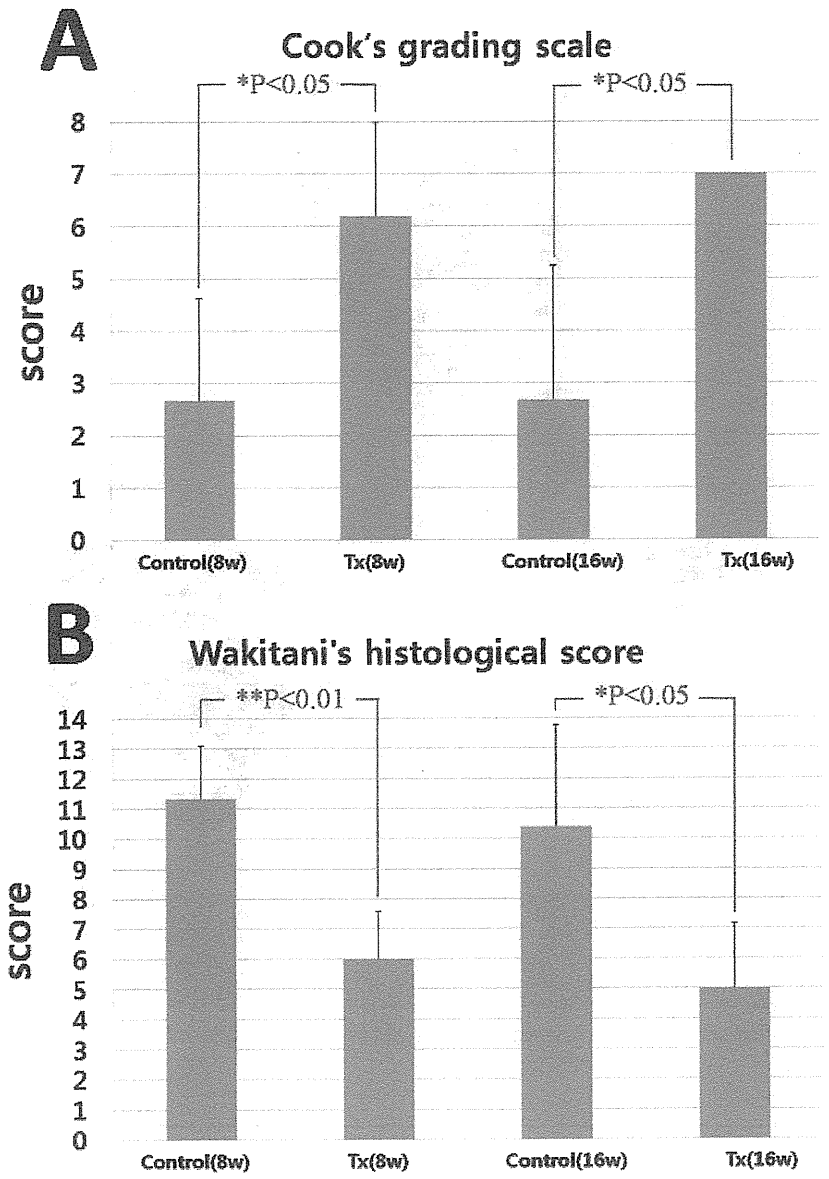

Fig. 5. Grading scores for gross and microscopic appearance. (**A**) Cook's scores. (**B**) Wakitani's histological scores.

11-12 days of continuous culture passaging, it was possible to trypsinise three times for ACs and five times for SYs. Ultimately, the third passage of ACs and the fifth passage of SYs were utilised to fabricate the scaffold-free spheroids (Fig. 2A). It has previously been reported that SYs have the characteristics of MSCs when isolated and cultured according to the method of primary culture described by (Koga *et al.*, 2007; Koga *et al.*, 2008a).

Proliferative capacity of ACs and SYs

The proliferative potency of the SYs was significantly greater than that of the ACs. The PGRs for the ACs and SYs were 0.51 ±0.11 and 0.96 ±0.29, respectively (Fig. 2B). The PGR for the SYs was approximately double that for the ACs.

Morphological analysis of spheroids

Analyses were performed with ACs and SYs derived from the third or fifth passage, respectively. Fig. 3A–D shows the changes in the appearance of representative cellular aggregates (75:25 SY:AC) with time among other SY:AC ratios under a phase contrast micrograph. The cells undergoing HDSS gathered into small numbers of cell clusters and anchored onto others over time. The surfaces of the cell aggregations gradually became smooth from an original rough state. The final diameters of the spheroids were ~250-700 μm, divided into two groups according to size. The smaller spheroids were ~250 ±100 μm and the larger spheroids were ~700 ±250 μm. The spheroidal cell aggregates were macroscopically observed within 12 h of HDSS (Fig. 3B–E). After 2-3 days of HDSS, the cellular aggregates were considered stable enough to be handled with micropipette aspiration (Fig. 3E, G–I).